Electronic Supplementary Material (ESI) for Physical Chemistry Chemical Physics.

Electronic Supplementary Information to Threshold Photoelectron Spectrum and Dissociative Photoionization of Benzonitrile

Jerry Kamer,[†] Domenik Schleier,[†,‡] Merel Donker,[†] Patrick Hemberger,[¶] Andras Bodi,[¶] and Jordy Bouwman[*,§,‖,⊥]

[†]*Laboratory for Astrophysics, Leiden Observatory, Leiden University, NL 2300 RA Leiden, The Netherlands*

[‡]*Lehrstuhl Technische Thermodynamik, Fakultät für Maschinenbau, Universität Paderborn, Warburger Str. 100, 33098 Paderborn, Germany*

[¶]*Laboratory for Synchrotron Radiation and Femtochemistry, Paul Scherrer Institut, 5232 Villigen, Switzerland*

[§]*Laboratory for Atmospheric and Space Physics, University of Colorado, Boulder, CO 80303, USA*

[‖]*Department of Chemistry, University of Colorado, Boulder, CO 80309, USA*

[⊥]*Institute for Modeling Plasma, Atmospheres and Cosmic Dust (IMPACT), NASA/SSERVI, Boulder, CO 80309, USA*

E-mail: Jordy.Bouwman@colorado.edu

Phone: +31715278432

This Electronic Supplementary Information contains further information to the main manuscript. First, an overview TPES of benzonitrile is presented. Next, the geometries of the $\widetilde{X}^+$, $\widetilde{B}^+$ and $\widetilde{C}^+$ excited states are shown with the bond lengths and angles, together with their Cartesian coordinates. Finally, a detailed description of the potential energy surface (PES) is provided.

TPES overview

The full threshold photoelectron spectrum of benzonitrile spanning the energy range from 9.5 to 14.0 eV is shown in Fig. S1.

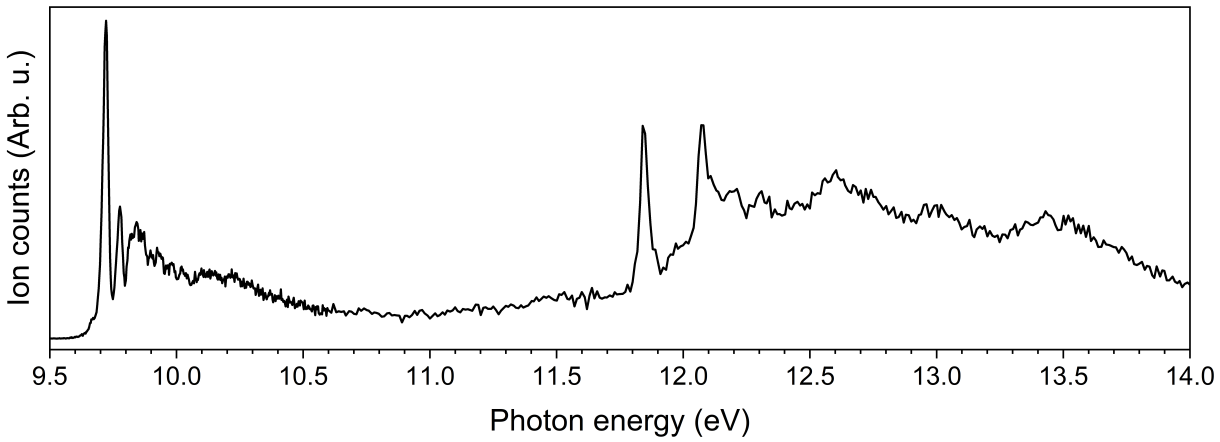

Figure S1: Threshold photoelectron spectrum of benzonitrile for the energy range of 9.5 to 14.0 eV.

Benzonitrile excited state structures and their Cartesian coordinates

In this section the Cartesian coordinates of the $\widetilde{X}^+$, $\widetilde{B}^+$ and $\widetilde{C}^+$ excited states that are used to simulate the TPES data are provided together with the bond lengths and angles. The structures were optimized using the ωB97XD/6-311++G(d,p) method.

Fig. S2 shows the geometry of the neutral ground state of benzonitrile. The structure is

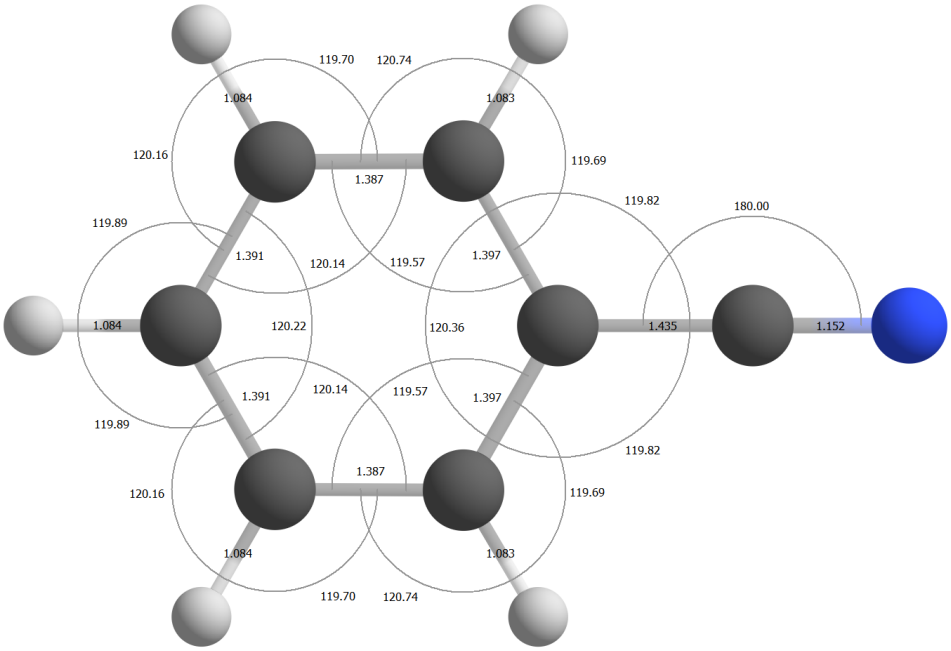

Figure S2: Molecular structure of the neutral ground state of benzonitrile accompanied with the bond lengths in Å and bond angles in degrees.

of C_{2v} symmetry. The Cartesian coordinates of this state are presented in Table 1.

Table S1: Cartesian coordinates of the molecular structure of the neutral ground state of benzonitrile.

Atom	Coordinates		
	x	y	z
C	0.000000	1.205814	−1.477156
C	0.000000	1.211771	−0.090012
C	0.000000	0.000000	−2.170236
H	0.000000	2.145173	0.459703
C	0.000000	0.000000	0.604488
C	0.000000	−1.205830	−1.477156
H	0.000000	−2.144650	−2.018109
C	0.000000	−1.211750	−0.090024
H	0.000000	−2.145189	0.459703
C	0.000000	0.000000	2.039246
N	0.000000	0.000000	3.190878
H	0.000000	0.000000	−3.254222
H	0.000000	2.144634	−2.018109

Fig. S3 shows the geometry of the $\widetilde{X}^+$ ground state of benzonitrile cation. The structure

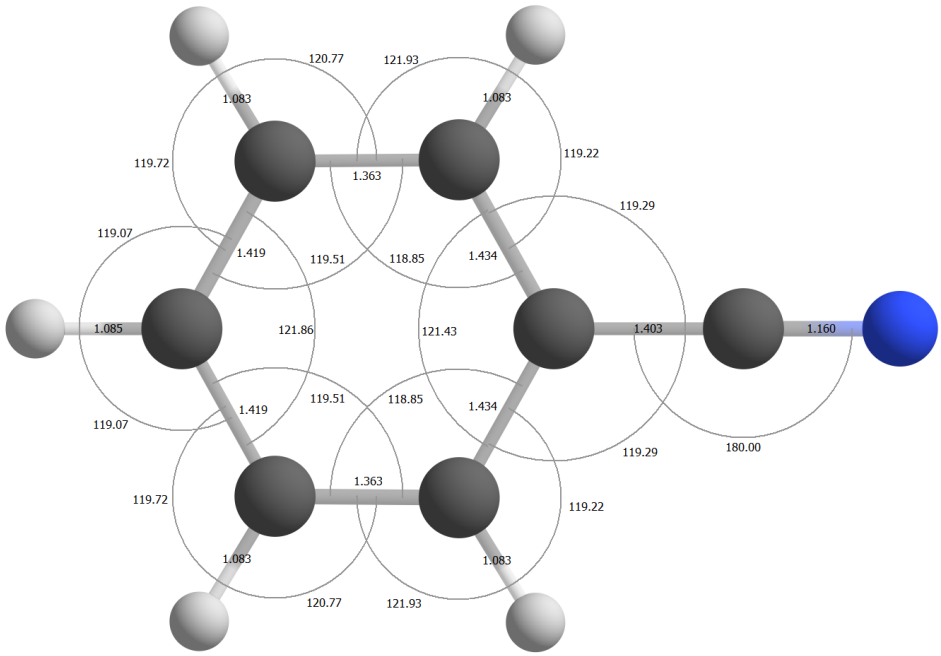

Figure S3: Molecular structure of the $\widetilde{X}^+$ excited state of benzonitrile accompanied with the bond lengths in Å and bond angles in degrees.

is of C_{2v} symmetry, similar to neutral benzonitrile. The Cartesian coordinates of this state are presented in Table 2 .

The geometry of the second excited state of the benzonitrile cation, the $\widetilde{B}^+$ state, is shown in Fig. S4. Most notably, compared to the $\widetilde{X}^+$ state, the phenyl ring is compressed perpendicular to the principal axis, thereby elongating the ring along this axis. Nevertheless, the structure remains in C_{2v} symmetry. Cartesian coordinates of the $\widetilde{B}^+$ state are presented in Table 3.

Lastly, Fig. S5 shows the geometry of the $\widetilde{C}^+$ state of benzonitrile. A significant structural change compared to the ground state ion is visible. The most apparent change is that the CN group now has a 179.66° angle. This, along with other structural changes, gives the geometry a C_s symmetry. The Cartesian coordinates of the $\widetilde{C}^+$ state are presented in Table 4 .

Table S2: Cartesian coordinates of the molecular structure of the cationic ground state of benzonitrile.

Atom	Coordinates		
	x	y	z
C	0.000000	1.240442	−1.458870
C	0.000000	1.250888	−0.095564
C	0.000000	0.000000	−2.148443
H	0.000000	2.174662	0.470353
C	0.000000	0.000000	0.605973
C	0.000000	−1.240442	−1.458870
H	0.000000	−2.166581	−2.019942
C	0.000000	−1.250888	−0.095564
H	0.000000	−2.174662	0.470353
C	0.000000	0.000000	2.009291
N	0.000000	0.000000	3.169308
H	0.000000	0.000000	−3.233685
H	0.000000	2.166581	−2.019942

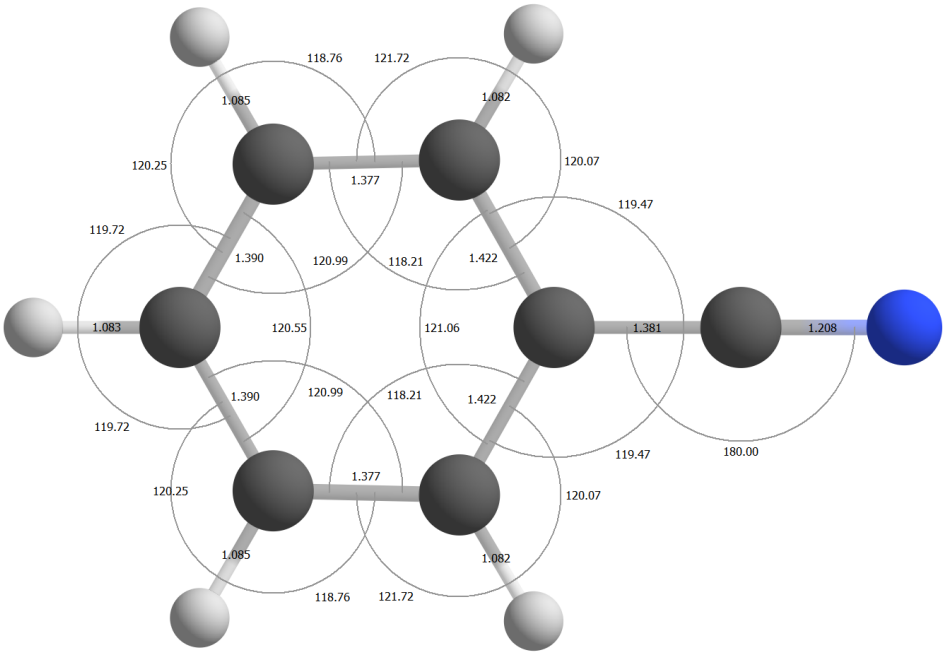

Figure S4: Molecular structure of the $\widetilde{B}^{+}$ state of benzonitrile accompanied with the bond lengths in Å and bond angles in degrees.

Table S3: Cartesian coordinates of the molecular structure of the $\widetilde{B}^{+}$ state of benzonitrile.

Atom	Coordinates		
	x	y	z
C	0.000000	1.207494	−1.467357
C	0.000000	1.237862	−0.090594
C	0.000000	0.000000	−2.156744
H	0.000000	2.170779	0.457956
C	0.000000	0.000000	0.608925
C	0.000000	−1.207490	−1.467357
H	0.000000	−2.146713	−2.010169
C	0.000000	−1.237872	−0.090570
H	0.000000	−2.170775	0.457956
C	0.000000	0.000000	1.989875
N	0.000000	0.000000	3.198174
H	0.000000	0.000000	−3.239851
H	0.000000	2.146717	−2.010169

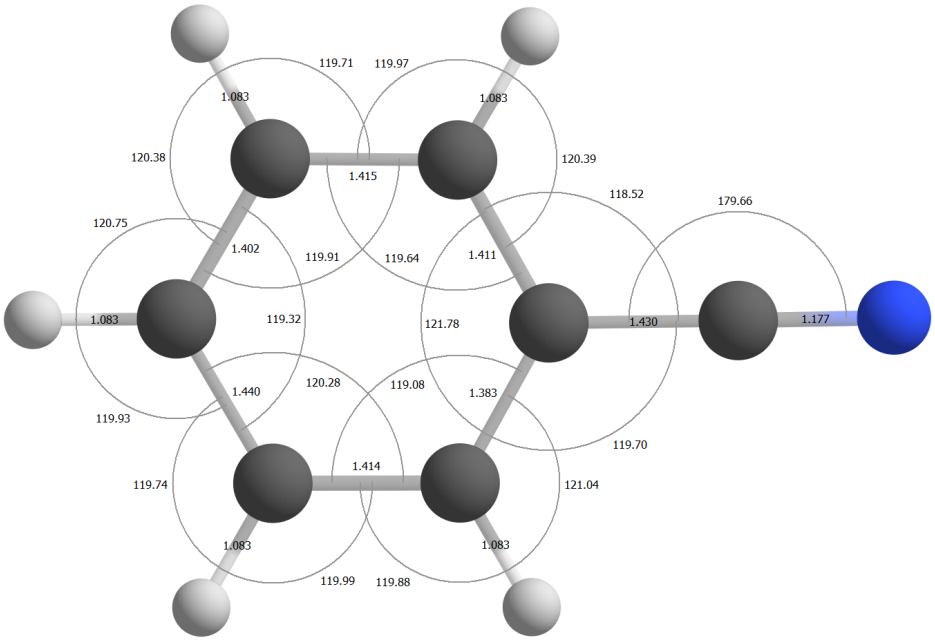

Figure S5: Molecular structure of the $\widetilde{C}^{+}$ state of benzonitrile accompanied with the bond lengths in Å and bond angles in degrees.

Table S4: Cartesian coordinates of the molecular structure of the $\widetilde{C}^{+}$ state of benzonitrile.

Atom	Coordinates		
	x	y	z
C	0.000000	1.271570	−1.441290
C	0.000000	1.228442	−0.028106
C	0.000000	0.050584	−2.204940
H	0.000000	2.150541	0.539895
C	0.000000	0.000000	0.606781
C	0.000000	−1.179716	−1.532533
H	0.000000	−2.108556	−2.089848
C	0.000000	−1.210675	−0.117513
H	0.000000	−2.160762	0.403006
C	0.000000	−0.059134	2.035740
N	0.000000	−0.114823	3.211320
H	0.000000	0.090139	−3.287217
H	0.000000	2.225972	−1.953906

Detailed description of the PES

This section gives an in-depth description of the PES presented in the main manuscript. To facilitate the description of the isomerization pathways, the carbon atoms are numbered as shown in Fig. S6. The pathways will be described in descending order of m/z of the cationic

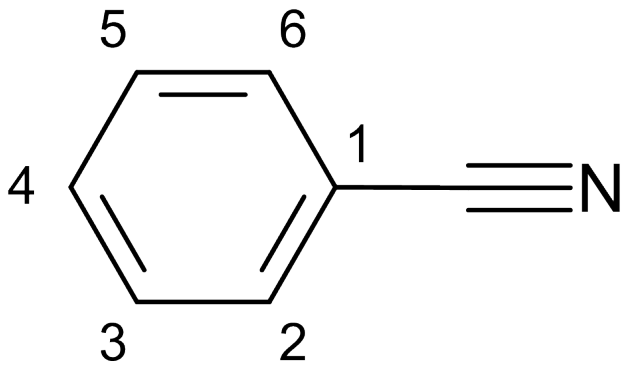

Figure S6: The molecular structure of benzonitrile (C_6H_5CN). The carbon atoms in the phenyl ring are numbered

fragments. The colors of the pathways match with the fragments in the breakdown diagram presented in the main manuscript. The pathways depicted in black are not considered in the breakdown diagram simulations.

CN loss comprises a benzonitrile dissociation channel in which the CN is removed without a reverse barrier (Fig. S7), resulting in the closed-shell phenylium$^+$ and CN$^\cdot$ at an energy of 4.34 eV, with respect to the benzonitrile cation ground state. This channel accounts for about 22% at an energy of 17.0 eV.

HCN loss is the dominant dissociation channel from the onset of dissociation up to about 18.1 eV. At a maximum it accounts for about 98% of the fractional abundance at around 15 eV. This channel leads to the formation of bicyclic *meta*-benzyne$^{\cdot+}$ (BMB$^{\cdot+}$) and HCN. The pathway leading to HCN loss is displayed in Fig. S7. The lowest energy path to HCN loss is found to start via **TS1**, which is direct H atom migration from C2 (or by symmetry C6) to the N atom by the at 3.42 eV. This also happens to be the rate-limiting step of the HCN loss channel. Optimizations were also done on the H atom migration to the C atom

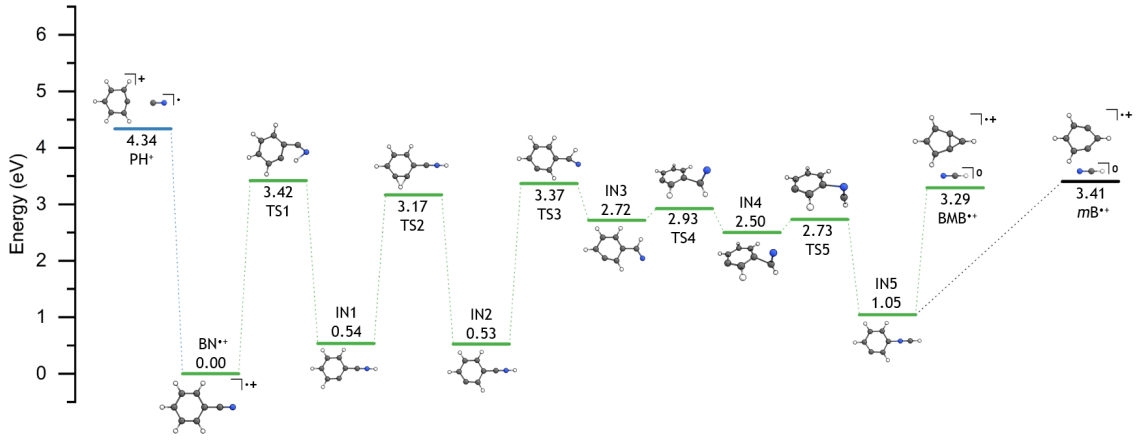

Figure S7: The benzonitrile$^{\cdot+}$ potential energy surface resulting in m/z 76 and 77 (blue). Both BMB$^{\cdot+}$ (green) and *meta*-benzyne$^{\cdot+}$ (black) are presented.

of the nitrile group, however the resulting structure does not converge and the H atom ends up on the N atom instead. The intermediate state **IN1**, formed over **TS1**, lies at an energy of 0.54 eV. From **IN1**, the H atom bound to C3 migrates to the vacancy on C2 via **TS2** at 3.17 eV, resulting in the intermediate state **IN2** at 0.53 eV. Subsequently, the H atom moves from the nitrogen to the carbon in the nitrile group, creating the HCN moiety. This transition state **TS3** sits at 3.37 eV and gives rise to the intermediate state **IN3** at 2.72 eV. Next, **TS4** located at 2.93 eV is crossed, resulting in **IN4** at 1.05 eV which has an HCN moiety perpendicular to the plane of the phenyl ring. From this intermediate state, the HCN moiety can connected with the nitrogen to C1 via **TS5** at 2.73 eV, resulting in **IN5** which sits at 1.05 eV. This structure exhibits the HCN moiety in-plane with the phenyl ring and the nitrogen atom bound to C1. Finally, bringing C3 and C6 together results in the energetically favorable $C_6H_4^{\cdot+}$ structure: BMB$^{\cdot+}$ + HCN at 3.29 eV. Alternatively, by elongating the N-C bond without bringing C3 and C6 closer the fragments *meta*-benzyne$^{\cdot+}$ and HCN are formed at 3.41 eV. Since both energies of the final products are below the energy of rate-limiting transition state **TS1** at 3.42 eV, both cationic fragments are potentially formed.

Ortho-benzyne is energetically unfavourable to be formed at the onset of HCN loss. At higher photon energies, however, *ortho*-benzyne could possibly be formed. The pathway is displayed in Fig. S8 and initially follows the same route as BMB$^{\cdot+}$ (or *meta*-benzyne$^{\cdot+}$)

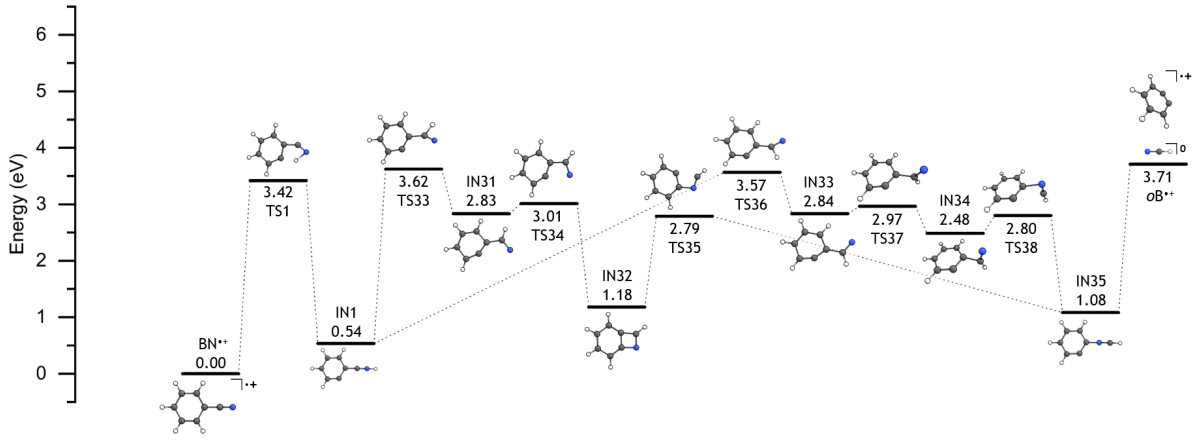

Figure S8: The benzonitrile$^{\bullet+}$ potential energy surface resulting in m/z 76 by forming *ortho*-benzyne$^{\bullet+}$. Two possible pathways are presented.

formation till **IN1**. Since, *ortho*-benzyne is being formed, no H atom migration in the phenyl ring is necessary. The H atom in the nitrile group moves from the nitrogen to the carbon, creating the HCN moiety. This can proceed in two fashions, namely by the H atom pointing away from the vacancy (**TS33**) or pointing towards it (**TS36**). Following **TS33** at 3.62 eV, we end up at **IN31** with an energy of 2.83 eV. The N atom moves towards the vacancy on the phenyl ring via **TS34** at 3.01 eV and binds to C2, resulting in the bicyclic molecule of **IN32** at 1.18 eV. Subsequently, the bond between C1 and the nitrile group opens which results in **IN35**, where the linear HCN group is bound to C2 with the nitrogen, at 1.08 eV. Separating HCN from the phenyl ring results in out-of-plane *ortho*-benzyne$^{\bullet+1}$ and HCN at 3.71 eV. Following **TS36** at 3.57 eV, we end up at **IN33** with an energy of 2.84 eV. Elongating the bond between C1 and the nitrile group, rotates the nitrile group via **TS37** at 2.97 eV, until it sits in the configuration of **IN34** at 2.48 eV. When the N atom moves towards C1 via **TS38** at 2.80 eV, it binds to C1 causing the C-C bond between C1 and the nitrile group to break, results in **IN35**. Now out-of-plane *ortho*-benzyne$^{\bullet+}$ and HCN can be formed by separating HCN from the phenyl ring. The formation of *ortho*-benzyne$^{\bullet+}$ from benzonitrile$^{\bullet+}$ proceeds without a reverse barrier.

HNC loss, depicted in Fig. 9, follows a similar trend as HCN loss for the first few transition and intermediate states. Contrary to HCN loss, at **IN1** and **IN2** the HNC group sepa-

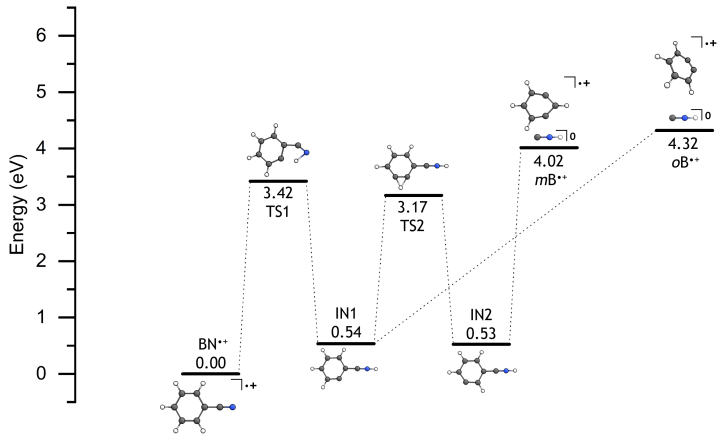

Figure S9: The benzonitrile$^{\bullet+}$ potential energy surface resulting in m/z 76 by loss of HNC. Both *meta*- and *ortho*-benzyne$^{\bullet+}$ are presented

rates from the molecule without any reconfiguration, resulting in *ortho*- and *meta*-benzyne$^{\bullet+}$ + HNC, respectively.

C_2H_4 loss is the only found dissociation pathway to result in a cationic fragment still containing the nitrogen atom of the nitrile group. Within the photon energy range used for this work, this channel does not reach its maximum fractional abundance. The final fragment being formed after dissociation are cyanodiacetylene$^{\bullet+}$ ($HC_5N^{\bullet+}$) and ethylene (C_2H_4). This pathway (shown in Fig. 10) starts by hydrogen migration from C6 to C1 via **TS6** at 2.52 eV. The subsequent intermediate state **IN6** sits at an energy of 2.17 eV, with both the migrated

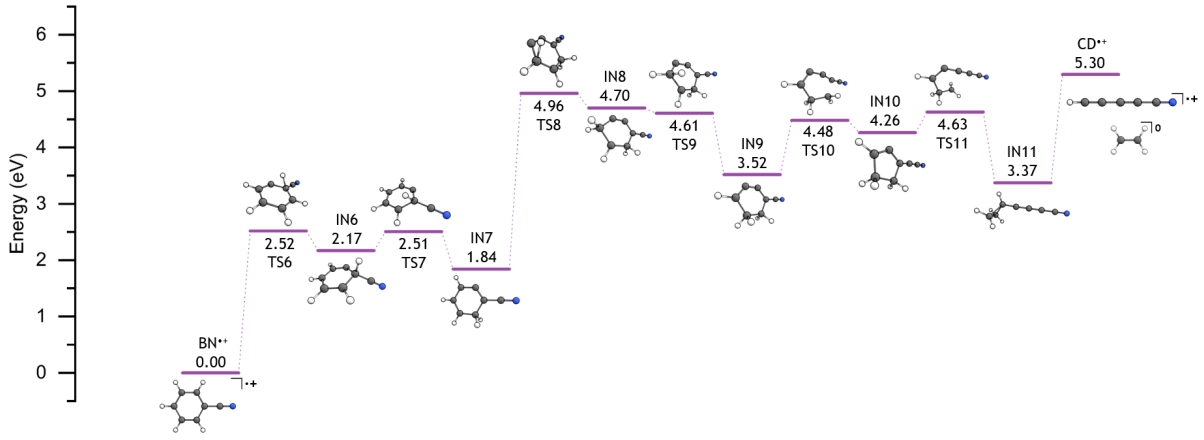

Figure S10: The benzonitrile$^{\bullet+}$ potential energy surface resulting in m/z 75 ($HC_5N^{\bullet+}$).

hydrogen and the nitrile group sticking out-of-plane. This hydrogen then migrates further

to C2 over **TS7** at 2.51 eV, resulting in **IN7** at 1.84 eV with both hydrogens at C2 now sticking out-of-plane. Now, the H atom at C5 migrates to C4, which results in 4.96 eV of required energy to traverse **TS8**, eventually ending up at intermediate state **IN8** at 4.70 eV. One of the hydrogens of C4 then migrates further to C3 via **TS9** at 4.61 eV to form the intermediate state **IN9** at 3.52 eV where two hydrogens sit on both C2 and C3 coming from C6 and C5, respectively. The computed CBS-QB3 energy for **IN8**, however, is slightly higher in comparison to **TS9**. Through the imaginary frequency of **TS9** it is confirmed that it indeed leads to **IN9**. CBS-QB3 utilizes the extrapolated wave function theory in order to determine the electronic energy of a molecular geometry, which is established by density functional theory. This can result in the calculated energy of a transition state being lower than that of the following intermediate state. **TS10** is subsequently traversed at 4.48 eV due to the bond breaking of C1 and C2, thus opening the phenyl ring. However, this ring is closed right after when C2 binds to C6, therefore creating the five-membered ring structure of **IN10** which sits at 4.26 eV. Breaking the bond between C2 and C6 via **TS11** at 4.63 eV, causes the ethylene group to rotate and to bind both C2 and C3 to C4, resulting in **IN11** at 3.37 eV. Separating the ethylene group from the molecule, results in the formation of cyanodiacetylene$^{\cdot+}$ and ethylene without a reverse barrier.

H_2CN loss is also considered in this section. The energy of this pathway (shown in Fig. 11) is 0.01 eV higher than the pathway to C_2H_4 loss and therefore deemed to not be energetically favourable. However, since the energy difference is so little it will be described here. H_2CN loss follows a similar path as HCN loss up to **IN5**, but from here an H atom migration occurs over **TS31** at 5.01 eV to form the intermediate **IN29** at 3.23 eV. Next, **IN30** at 3.02 eV is formed over **TS32** at 4.69 eV. Lastly, by elongating the C–N bond in **IN30**, *c*-$C_6H_3^+$ and $H_2CN^{\cdot}$ are obtained at 5.31 eV. This is also the rate-limiting step and takes place without a reverse barier.

HC_3N loss shows up in the mass spectra at m/z 52 at relatively low photon energy (15.7 eV). The lowest pathway found leads to the formation of methylene-cyclopropene$^{\cdot+}$ +

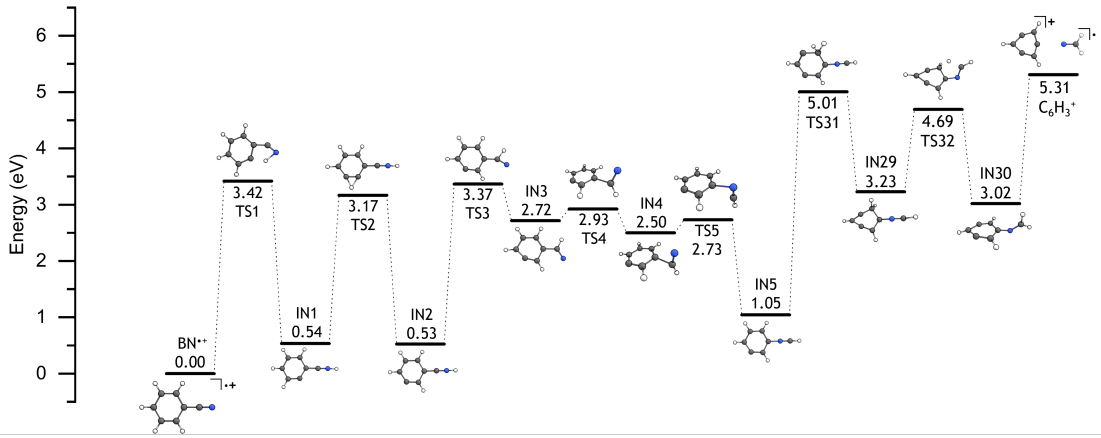

Figure S11: The benzonitrile$^{\bullet+}$ potential energy surface resulting in m/z 75 (c-$C_6H_3^+$).

cyanoacetylene. The mechanism is shown in Fig. S12 and starts by the H atom migration from C4 to C3, crossing **TS12** at 2.20 eV and resulting in **IN12** at 1.82 eV. The next step is to break the C1 and C6 bond and cross **TS13** which is the rate-limiting transition state corresponding to ring opening and is located at 3.69 eV, resulting in **IN13** at 3.13 eV. Next, a rotation takes place around the C2–C3 bond via **TS14** at 3.19 eV, resulting in **IN14** at 3.19 eV. From here, the C2 and C3 bond can be broken by elongation, over **TS15** at 4.14 eV, resulting in methylene-cyclopropene$^{\bullet+}$ and cyanoacetylene at 4.04 eV. **TS15** happens to be the rate-limiting step of this dissociation pathway.

H_2C_3N loss (shown in Fig. S12) leads to the formation of $H_2C_4H^+$ at m/z 51 and cyanovinyl$^{\bullet}$, and follows the same initial step as the HC_3N loss channel. However, instead of ring opening from **IN12**, an H atom on C3 moves to C2 via **TS16** at 2.27 eV. This results in **IN15** at 1.82 eV. Next, the H atom on C5 migrates towards the neighboring C6 over **TS17** at an energy of 4.78 eV and results in **IN16** at 4.09 eV. Ring opening at C2 and C3 over **TS18** 5.25 eV results in **IN17** at 3.81 eV. From here, **IN18** at 2.63 eV is formed over **TS19** at 4.15 eV. An internal rotation around the C–C bond takes place via **TS20** at 3.00 eV, resulting in **IN19** at 2.54 eV. By elongating said C–C bond, the transition state **TS21** is traversed at 5.07 eV, which results in **IN20** at 4.74 eV, where the molecule only has an N–H bond. Breaking this bond results in the formation of the two fragments at 5.40 eV.

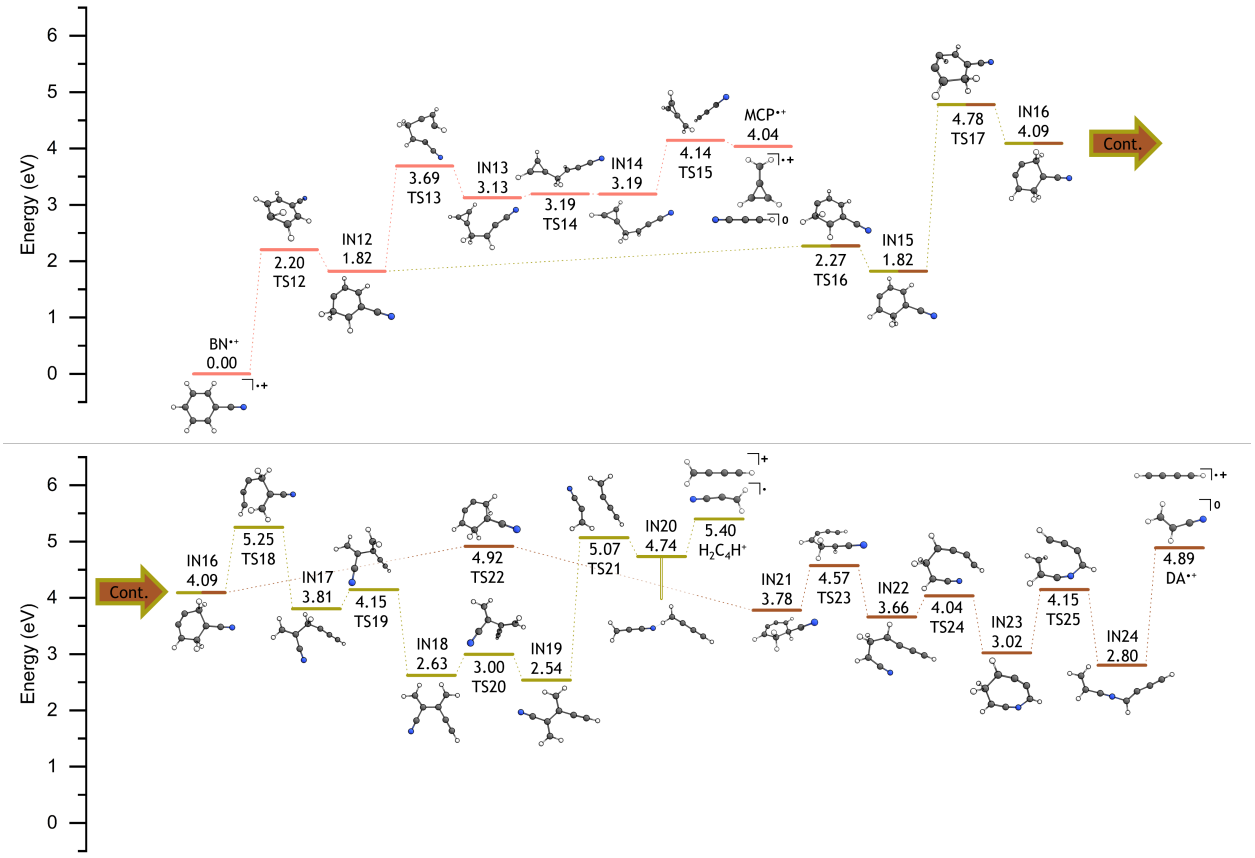

Figure S12: The benzonitrile$^{\cdot+}$ potential energy surface leading to the m/z 50 (brown), 51 (yellow), and 52 (orange) fragment ions.

CH_2CHCN loss is the dominant dissociation channel from 18.1 eV onward and results in an ion with m/z 50 that exhibits a maximum of about 30% around 19.75 eV. The final products found for this channel are diacetylene$^{\cdot+}$ and acrylonitrile, and the pathway is displayed in Fig. S12. This loss channel shows a similar lowest energy pathway to H_2C_3N loss. Instead of ring opening from **IN16**, however, it proceeds via hydrogen migration of C6 to C1 over **TS22** at 4.92 eV to form **IN21** at 3.78 eV. Next, bond breaking of C1 and C6 ensures the ring opening via **TS23** at 4.57 eV resulting in **IN22** at 3.66 eV. Subsequently, a new ring is formed by moving the nitrogen to C6 via **TS24** at 4.04 eV resulting in **IN23** at 3.02 eV. The newly formed ring is broken by the rupture of the C2 and C3 bond via **TS25** at 4.15 eV, forming intermediate **IN24** at 2.80 eV. Finally, breaking the C–N bond results in diacetylene$^{\cdot+}$ and acrylonitrile at 4.89 eV.

H_2C_4N loss results in the formation of cyclopropenium$^+$ (at m/z 39) and $H_2C_4N^{\cdot}$ and is schematically displayed in Fig. S13. This pathway starts by H atom migration from

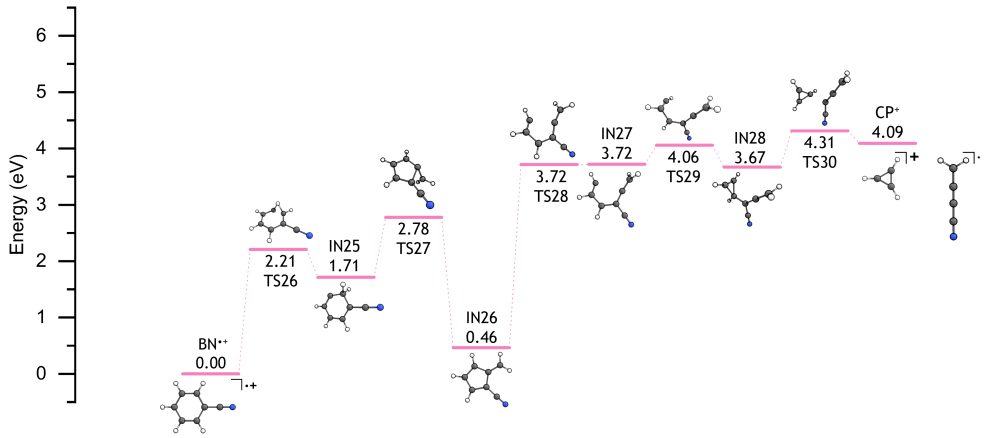

Figure S13: The benzonitrile$^{\cdot+}$ potential energy surface resulting in m/z 39.

C5 to C6 over **TS26** at 2.21 eV, resulting in **IN25** at 1.71 eV. Ring compression over **TS27** at 2.78 eV, results in the formation of the five-membered ring intermediate **IN26** at 0.46 eV. Subsequently, ring opening occurs over **TS28** at 3.72 eV and results in intermediate **IN27** at similar energy. Next, **TS29** at 4.06 eV is crossed, resulting in **IN28** at 3.67 eV. Lastly, separating the cyclic species from the H_2C_4N moiety via **TS30** at 4.31 eV, results in cyclopropenium$^+$ + $H_2C_4N^{\cdot}$ at 4.09 eV.

(Bicyclic) *meta*-benzyne molecular orbitals

Molecular orbitals (MOs) of *meta*-benzyne and bicyclic *meta*-benzyne (BMB) will be presented in this section. Fig. 14 displays the singly occupied MO (SOMO) of the *meta*-benzyne and BMB cations, and the highest occupied MO (HOMO) and HOMO−1 of neutral *meta*-benzyne. The *meta*-benzyne and BMB cation SOMOs are clearly different, and show a $^2A_1$

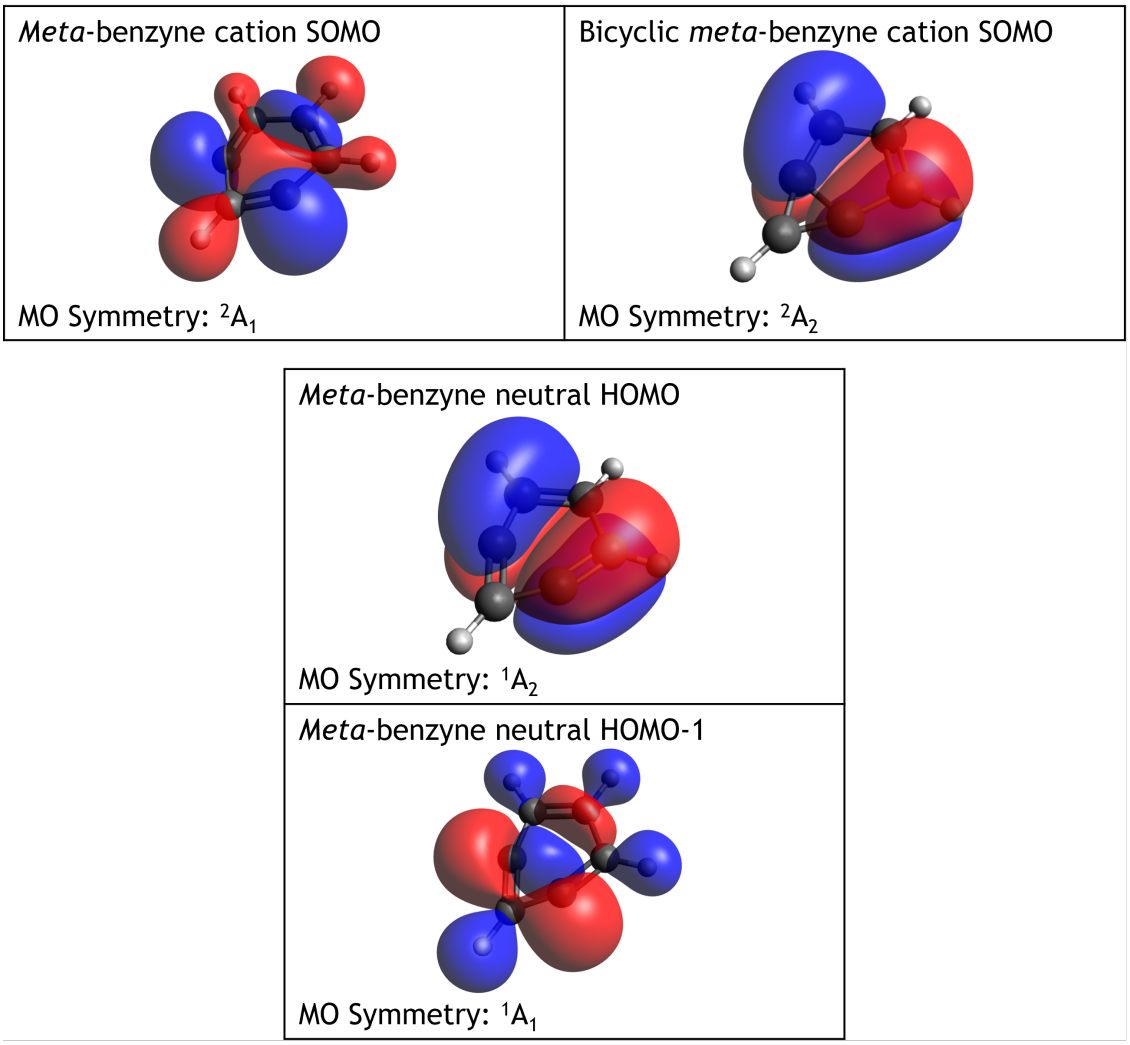

Figure S14: The SOMO of the *meta*-benzyne and BMB cations, and the HOMO and HOMO−1 of neutral *meta*-benzyne.

and $^2A_2$ symmetry, respectively. Thus, the two cationic isomers represent two minima with different wave function symmetries and are therefore clearly distinguishable. It seems that ionization out of the neutral HOMO leads to the BMB cation, while ionization out of the

HOMO−1 results in the *meta*-benzyne cation.

References

(1) Kaiser, D.; Reusch, E.; Hemberger, P.; Bodi, A.; Welz, E.; Engels, B.; Fischer, I. The *ortho*-benzyne cation is not planar. *Phys. Chem. Chem. Phys.* **2018**, *20*, 3988–3996.